



ELSEVIER

Contents lists available at ScienceDirect

Materials Letters

journal homepage: www.elsevier.com/locate/matlet

Microstructure of Fe₂O₃ scaffolds created by freeze-casting and sintering



Ranier Sepúlveda^{a,*}, Amelia A. Plunk^b, David C. Dunand^b

^a Department of Engineering and Materials Science, E.T.S. de Ingenieros, Universidad de Sevilla, Avda. Camino de los Descubrimientos s/n., 41092 Sevilla, Spain

^b Department of Materials Science and Engineering, Northwestern University, Evanston, IL 60208, USA

ARTICLE INFO

Article history:

Received 9 September 2014

Accepted 29 November 2014

Available online 4 December 2014

Keywords:

Freeze-casting

Fe₂O₃

Camphene

Hydrogen

Porous materials

Redox process

ABSTRACT

Fe₂O₃ scaffolds with an open porosity of ~81% were fabricated by freeze casting of a suspension of hematite nano-particles in liquid camphene, sublimation of the camphene, and sintering of the interconnected walls of hematite particles concentrated in the interdendritic spaces. At high solidification velocity, the camphene dendrites created, after sublimation, equiaxed, interconnected macropores, whose size increases with decreasing velocity and which are surrounded by interconnected hematite walls. At the lowest solidification velocity, camphene dendrites grow radially into the sample along the temperature gradient, creating, after sublimation, aligned elongated macropores, 50–150 μm in diameter and 3–4 mm in length, surrounded by aligned hematite walls with low levels of microporosity after sintering. Hydrogen reduction of such a sample resulted in a metallic iron scaffold with the same elongated macropore and densified iron walls.

© 2014 Elsevier B.V. All rights reserved.

1. Introduction

The use of hydrogen as a large-scale energy carrier is hampered by its difficult storage, transportation and supply [1]. The reversible steam/hydrogen redox reactions between iron oxide and iron to produce and store hydrogen have emerged as a low-cost, scalable solution to these issues [2]. However, multiple redox cycles on beds of iron oxide powders result in their sintering and a concomitant reduction in hydrogen storage/production capacity [3]. As an alternative, it is proposed here to use an iron oxide scaffold, which is expected to have a lower tendency to sinter during cyclical redox reactions due to its interconnected, highly porous structure.

A scalable, low-cost method to create ceramic scaffolds is a freeze-casting technique which relies on the solidification of a liquid phase in which particles or powders have been dispersed [4]. As dendrites grow during solidification, they push and concentrate the suspended particles in the interdendritic spaces. Sublimation of the solidified phase leaves a green powder scaffold, whose struts or walls are then sintered at elevated temperature. Porous structures can be designed by altering the particles characteristics and concentration, the solidification direction and velocity, and the liquid medium [5]. This technique has been extensively used for

submicron ceramic powders using water [6] or camphene [7] as media, as well as for coarser titanium powders [8]. Recently, the freeze-casting of nanometric copper oxide particles suspended in water [9] or camphene [10] followed by hydrogen reduction has been demonstrated to produce a metallic (copper) scaffold but never date to produce iron, to our knowledge.

Here, we demonstrate, for the first time, that iron oxide (hematite, Fe₂O₃) scaffolds can be created by directional freeze-casting of camphene/hematite nanoparticle suspensions followed by camphene sublimation, and these scaffolds can be reduced to iron without degradation of the scaffold architecture. The hematite pore and wall microstructures are studied as a function of the casting temperature, which controls the dendrite solidification velocity.

2. Experimental procedures

Commercially available hematite powder (Fe₂O₃, from US Research Nanomaterials) with an average size of 20–40 nm was used. Camphene (C₁₀H₁₆, melting point of 48–52 °C, from Sigma-Aldrich) was used as media. An acrylic copolymer (Zephyrym PD 4913-LQ-(MV), from Croda Iberica) acted as dispersant agent. Polystyrene (PS, [CH₂CH(C₆H₅)]_n, from Sigma-Aldrich) with a molecular weight of 350,000 g/mol was added as a binder.

* Corresponding author.

E-mail address: rsepulveda@us.es (R. Sepúlveda).

A well-dispersed suspension of 5 vol% hematite in liquid camphene, to which 1 wt% of dispersant and 20 vol% of binder were added, was obtained using an ultrasonic water bath for 1 h at 60 °C. An 8 cm³ volume of suspension was prepared and then poured to fill a mold (20 mm in diameter and 25 mm in height) made with an alumina tube and a 0.2 mm thick PVC foil at its bottom. The mold was fixed on top of a thermally insulating expanded polystyrene (EPS) board and surrounded by a water bath at constant temperature (Fig. 1a), to promote radial, directional solidification. After casting the suspension, the mold was covered immediately with a 4 mm thick insulating PMMA sheet and the suspension was solidified for 24 h at one of four temperatures (30, 35, 40 and 42.5 °C) to determine the influence of the freezing velocity.

Solidified samples were subjected for 48 h to a forced air flow at room temperature (20 °C) to allow camphene sublimation. Green samples were then transferred to an alumina crucible and underwent a two-step heat treatment (Fig. 1b): (i) organic burn-out at 600 °C, and (ii) sintering of the Fe₂O₃ walls at 1100 °C. Furnace-cooling was used to prevent cracking due to thermal shocks. Sintered

samples (Fig. 1c) were easily handled and showed significant volume reduction, few faint radial cracks and a small dimple at the top surface at the last point of camphene solidification.

The fabricated samples were characterized by optical (OI, Nikon Epihot 200) and scanning electron microscopy (SEM, JEOL 6460LV) to evaluate the influence of the freezing velocity on the pore structure development. SEM images were analyzed using the ImagePro[®] software. The average density of the Fe₂O₃ walls (from which their closed porosity was calculated) was measured on the sintered samples using a Micromeritics AccuPyc II 1340 Helium Pycnometer, and their open porosity was determined by the Archimedes method, after soaking in hot water for 5 h followed by a 24 h immersion in cold water.

To demonstrate the creation of a metallic iron scaffold by hydrogen reduction, temperature-programmed reduction (TPR) experiments were performed on a 0.35 g section of a Fe₂O₃ sample, directionally solidified at 42.5 °C and sintered at 1100 °C, using a Micromeritics Autochem II 2920 under a flow of 10% H₂/bal Ar (20 ml/min) as follows: heated at 2 °C/min to 600 °C with a

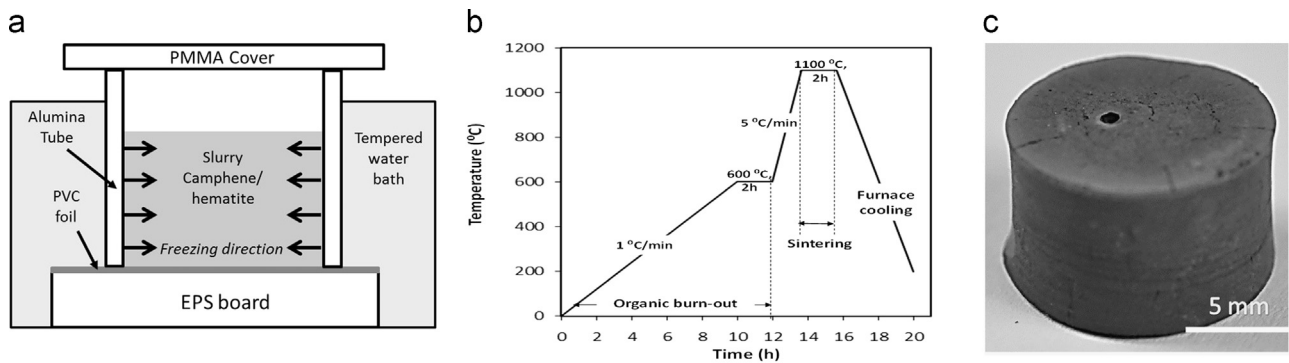


Fig. 1. (a) Schematic diagram of the experimental setup used for freeze casting. (b) Heat-treatment profile designed for burning out organic phases and sintering the Fe₂O₃ walls. (c) Sintered Fe₂O₃ sample from green sample solidified at 40 °C.

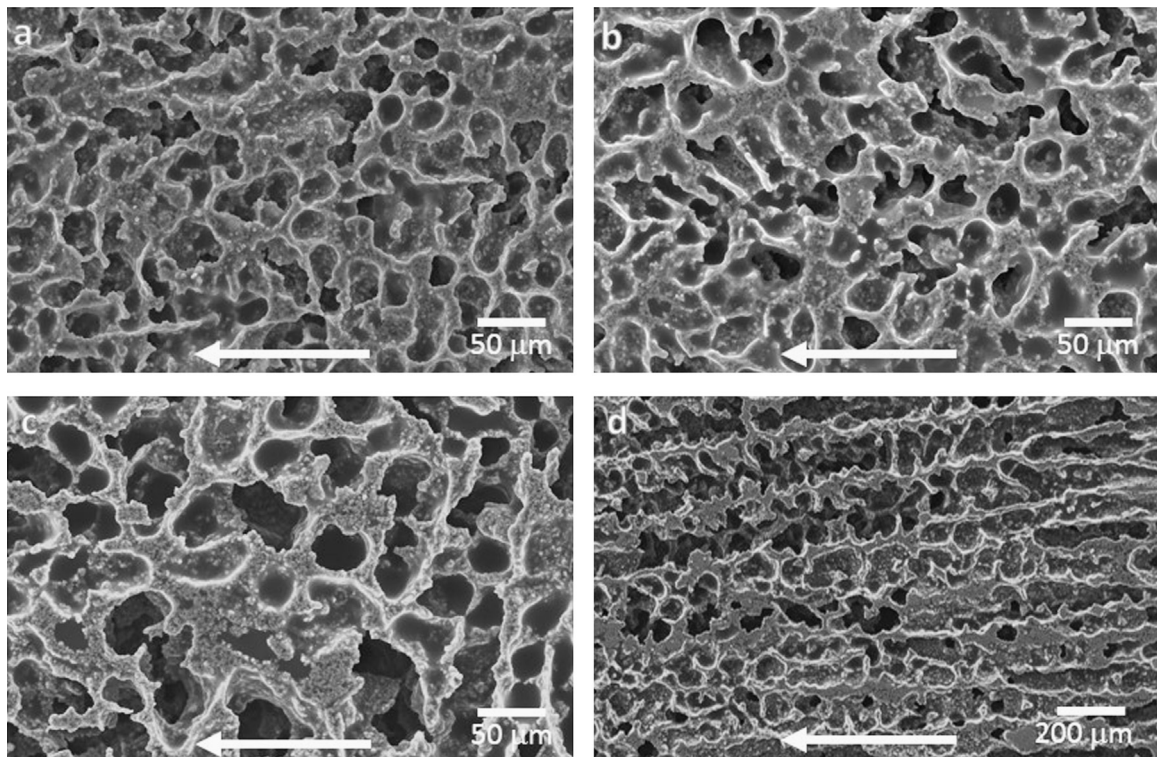


Fig. 2. SEM micrographs of radial cross-sections, taken mid-height within the sintered porous hematite scaffolds created at various freezing temperatures: 30 °C (a), 35 °C (b), 40 °C (c) and 42.5 °C (d). Arrows indicate the solidification direction.

dwelt time of 8 h, then heated at 10 °C/min to 900 °C with dwelt time of 2 h, followed by furnace cooling.

3. Results and discussion

Fig. 2 shows a series of SEM micrographs of the sintered samples solidified at the four different temperatures. The micrographs show a middle-height cross-section surface parallel to the radial solidification directions. Solidification temperatures at 30–40 °C produced a scaffold-like porous microstructure with near equiaxed pore shapes (Fig. 2a–c); by contrast, at a solidification temperature of 42.5 °C, elongated pores are obtained, which are aligned radially along the solidification direction (Fig. 2d). At this solidification temperature, the highest studied here, the solidification front velocity is sufficiently low to create fewer and highly aligned camphene dendrites, which pushed the hematite particles into the interdendritic spaces thus forming, after sublimation and sintering, radially oriented elongated pores. Indeed, 42.5 °C is in the range of temperatures quoted in the literature to produce such elongated porous structures with camphene [11], albeit with different particle size, fraction and composition. By contrast, at the lower freezing temperatures and faster solidification rates studied here, dendrites are expected to nucleate in higher number and to grow non-directionally before rapidly impinging on each other. The powders are pushed into the interdendritic spaces, resulting, after sublimation and sintering, in a continuous scaffold with isotropically-oriented walls as shown in Fig. 2a–c.

All sintered samples showed good densification of the solid walls, as reported in Table 1 with pycnometric densities close to the theoretical value for hematite (5.24 g/cm³). The closed porosity was markedly reduced when samples were solidified at the highest temperature of 42.5 °C (the lowest solidification rate), probably because particles packed more efficiently in the interdendritic space. The total porosity (closed and open porosities combined) was almost constant (83–84% in Table 1) regardless of the solidification temperature and the pore structure as expected. These values are lower than the original camphene volume fraction (95%) due to partial camphene

evaporation during sample fabrication, and the volume shrinkage following sintering. Neither distortion nor extensive cracking was detected on sintered samples despite a very large, 67–71%, volume change due to sintering. Table 1 also reports pore diameters and wall thicknesses, both measured by image analysis over several optical images taken across the central axial plane of the sintered samples. The morphological analysis shows an increase in pore diameter and scaffold wall thickness with an increase in solidification temperature. This is attributed to the lower rate of dendrite nucleation events with decreasing undercooling and concomitant larger dendrite and interdendritic sizes due to lower solidification rates. For the samples solidified at 42.5 °C the camphene dendrites grew directionally, creating elongated pores, 50–150 μm in diameter and 3–4 mm in length. No substantial variations of the pore diameter or wall thickness were detected within the sintered samples.

According to literature [12], Fe₂O₃ hydrogen reduction usually shows a well-defined two-step reaction, the first at ~270 °C and the second at ~350 °C, which correspond to reduction of Fe₂O₃ to Fe₃O₄, and Fe₃O₄ to Fe, respectively. TPR profiles of the scaffold solidified at 42.5 °C, sintered at 1100 °C and hydrogen-reduced at 900 °C (Fig. 3a) showed a shift to higher temperatures and the overlapping of the two consecutive reactions. This is consistent with a sintering process modifying the reduction kinetics probably from chemical (loose nano-size powders) to diffusion (dense micron-size struts) reaction controlling mechanism. Moreover, mass loss measurements of the scaffold were consistent with full reduction to metallic iron after heat treatment. The elongated pore structure was retained although its size was reduced due to the significant sample volume reduction associated with the hematite reduction (Fig. 3b). The reduced metallic iron walls (Fig. 3c) are mostly sintered, showing 15.7% closed porosity as determined by helium pycnometer measurements. Such porosity may represent prior hematite micropores which were not sintered and/or new pores created from the oxygen loss and steam production during the reduction step.

4. Conclusions

Fe₂O₃ scaffolds with 83% porosity were created by freeze casting of a suspension of nanometric hematite particles in liquid camphene followed by camphene sublimation and air sintering. During solidification, camphene dendrites push the particles into interdendritic spaces and subsequent sublimation of the dendrites creates two pore structures. At high solidification rates, macropores are equiaxed in shape, while at lower rates, they exhibit highly elongated shapes, aligned radially in the direction of the temperature gradient. Hydrogen reduction of the sintered hematite scaffold was demonstrated to create an iron scaffold with the same elongated pore structure and nearly dense metallic walls.

Table 1
Final volume change ($\Delta V/V$), wall density, porosity values and pore morphology of Fe₂O₃ sintered scaffolds fabricated at different solidification temperatures.

Solidification temperature (°C)	30	35	40	42.5
$\Delta V/V$ (%)	67	67	71	69
Wall density (g/cm ³)	5.12	5.13	5.12	5.17
Porosity (%): close/open	2.3/81.6	2.1/81.2	2.3/80.5	1.3/81.4
Pore diameter (μm)	20 ± 7	26 ± 9	35 ± 9	110 ± 28
Wall thickness (μm)	4 ± 3	7 ± 4	9 ± 5	15 ± 10

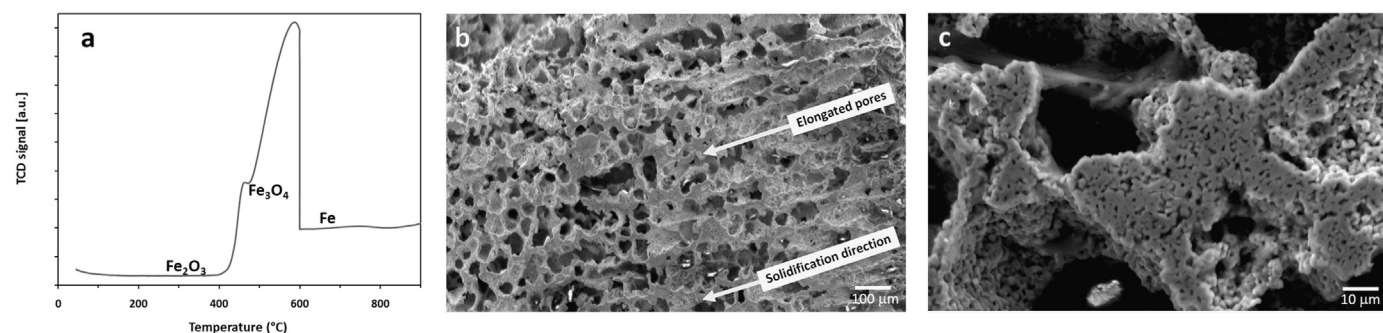


Fig. 3. (a) Hydrogen temperature programmed reduction (TPR) profiles of air-sintered Fe₂O₃ sample solidified at 42.5 °C. (b) SEM micrograph of the surface after reduction to iron. (c) Higher magnification view, showing micropores within the iron scaffold walls.

Acknowledgments

RS acknowledges support of Universidad de Sevilla. AP was supported by the National Science Foundation through a Graduate Research Fellowship under Grant no. DGE-1324585. DCD acknowledges support from the Institute for Sustainability and Energy at Northwestern.

References

- [1] Thomas JM, Raja R. Designing catalysts for clean technology, green chemistry, and sustainable development. *Annu Rev Mater Res* 2005;35:315–50. <http://dx.doi.org/10.1146/annurev.matsci.35.102003.140852>.
- [2] Thaler M, Hacker V. *Int J Hydrog Energy*. 2012;37:2800–6.
- [3] Romero E, Soto R, Durán P, Herguido J, Peña JA. *Int J Hydrog Energy* 2012;37:6978–84.
- [4] Deville S. *Adv Eng Mater* 2008;10:155–69.
- [5] Li WL, Lu K, Walz JY. *Int Mater Rev* 2012;57:37–60.
- [6] Waschkies T, Oberacker R, Hoffmann MJ. *Acta Mater* 2011;59:5135–45.
- [7] Lee E-J, Koh Y-H, Yoon B-H, Kim H-E, Kim H-W. *Mater Lett* 2007;61:2270–3.
- [8] Li JC, Dunand DC. *Acta Mater* 2011;59:146–58.
- [9] Ramos AIC, Dunand DC. *Metals* 2012;2:265–73.
- [10] Oh ST, Chang SY, Suk MJ. *Trans Nonferrous Met Soc China (Engl Ed)* 2012;22:s688–s691.
- [11] Yook SW, Kim HE, Koh YH. *Mater Lett* 2009;63:1502–4.
- [12] Pineau A, Kanari N, Gaballah I. *Thermochim Acta* 2006;447:89–100.